

INTEGRITY ASSESSMENT OF REVERSE ENGINEERED Ti-6Al-4V ELI TOTAL HIP REPLACEMENT IMPLANT

PROCENA INTEGRITETA Ti-6Al-4V ELI IMPLANTA ZA TOTALNU ZAMENU ZGLOBA KUKA KORIŠĆENJEM POSTUPKA REVERZNOG INŽENJERINGA

Originalni naučni rad / Original scientific paper
UDK /UDC: 616.728.2-77

Rad primljen / Paper received: 4.12.2019

Adresa autora / Author's address:

¹⁾ University of Belgrade, Innovation Centre of the Faculty of Mechanical Engineering, Belgrade, Serbia
email: amilovanovic@mas.bg.ac.rs

²⁾ University of Belgrade, Faculty of Mechanical Engineering, Belgrade, Serbia

³⁾ University of Belgrade, Faculty of Technology and Metallurgy, Belgrade, Serbia

Keywords

- total hip replacement implant
- finite element method (FEM)
- Ti-6Al-4V ELI alloy
- reverse engineering
- 3D scanner 'Geomagic Capture'

Abstract

Total hip replacement implants are used as an artificial replacement for dysfunctional hips in order to sustain joint movement. Chosen material and design of total hip replacement are the most influential factors for artificial joint utilization. Selected total hip replacement is obtained by precision casting method, made from Ti6Al4V ELI (Extra Low Interstitials) alloy. In order to acquire a geometrical model of chosen implant, the 3D scanner is used and an obtained point cloud (PC), then exploited for reverse engineering to a CAD model. The neck thickness of implant affects angle of movement of the joint and structural integrity. Reducing the thickness of the neck section results in higher movement of the joint, but inversely affects its structural integrity. The 3D scanned implant has a neck thickness of 14.6 mm, and data from literature suggest that the best movement angle is for 9 mm thickness of the implant. In order to redesign the available implant, five different models with a neck thickness between 9 and 14.6 mm are made. Obtained results show the thickness effects the stress distribution in a critical area.

INTRODUCTION

The function of total hip replacement is to carry the load induced by normal everyday activity. Loads that occur on total hip replacement implants can be as high as 8.7 times the body weight of a patient, which is the case of stumbling. Total hip replacement failure may be caused by implant loosening, wear of material, or fatigue, /1, 2/. During exploitation, these implants are under dynamic loading. Hence, the most probable mechanism of failure is fatigue. If defects, such as inclusions and micro cracks of total hip replacement implant are neglected, fatigue crack initiation is most probable at locations of maximal stress state. Areas around the implant neck carry the load and are an important aspect in the design of implant, /1, 3/. Thus, stress and strain analysis is very important, be it experimental or numerical, /1-6/.

Ključne reči

- implant za totalnu zamenu zgloba kuka
- metoda konačnih elemenata (FEM)
- Ti-6Al-4V ELI legura
- reverzno inženjerstvo
- 3D skener 'Geomagic Capture'

Izvod

Implanti za totalnu zamenu zgloba kuka se koriste kao veštačka zamena za disfunkcionalni kuk, kako bi se održalo kretanje zgloba. Za upotrebu implanta, najvažniji faktori su odabrani materijal i dizajn implanta. Odabrani implant je dobijen metodom preciznog livenja od legure Ti6Al4V ELI (ELI-niska koncentracija intersticijskih atoma). Kako bi se dobio geometrijski model odabranog implanta koristi se 3D skener i učitani oblak tačaka, koji je zatim poslužio za reverzni inženjering do CAD modela. Debljina vrata implanta utiče na maksimalni ugao kretanja kao i na integritet konstrukcije. Manje debljine vrata omogućavaju veći ugao kretanja implanta, ali nepovoljno utiču na integritet konstrukcije. 3D skenirani implant ima debljinu vrata 14,6 mm, a podaci iz literature sugerišu da je najbolje kretanje implanta kada je debljina vrata 9 mm. Kako bi se izvršio redizajn skenirane proteze, napravljeno je pet različitih modela sa debljinama vrata između 9 i 14,6 mm. Dobijeni rezultati pokazuju kako promena u debljini vrata proteze utiče na raspodelu napona u kritičnoj oblasti implanta.

Total hip replacement implant consists of stem, inserted in femur bone, and head that is placed onto the stem. The other component of a hip joint is UHMWPE (Ultra High Molecular Weight Polyethylene) cup with a metal back, inserted in acetabulum. Movement between UHMWPE cup and head make a hip joint. For a wider angle of movement of a hip joint, the implant neck needs to be as thin as possible. Literature data show that at 9 mm neck thickness the oscillation angle of the hip joint is at 56°, and at 12 mm oscillation, the angle decreases by 5°, /1, 2, 7/.

The selected total hip replacement implant, Fig. 1, is made from Ti-6Al-4V ELI by precision casting method. This alloy has a high strength-to-weight ratio (i.e. specific strength), corrosion resistance, durability and excellent biocompatibility - which makes this material a most widely used alloy in total hip replacement manufacture, /2, 7/. The neck thickness

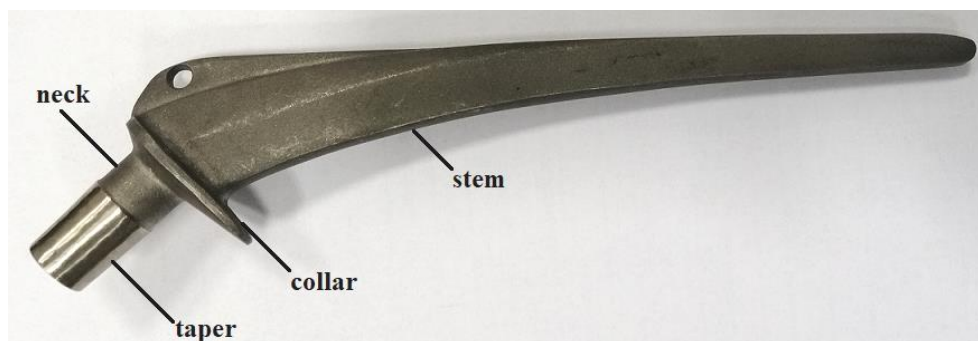


Figure 1. Selected total hip replacement implant.

of particular implant is 14.6 mm, providing long structural life of the implant at a cost of lower oscillation angle, i.e. worse hip joint movement. This research includes a possible redesign of the chosen implant in order to increase hip joint movement using Finite Element Analysis (FEA) to demonstrate how redesign will affect structural life of the component. Reverse Engineering (RE) method is used as a tool to obtain the CAD model of the selected implant and to manipulate the geometry.

REVERSE ENGINEERING

Reverse engineering is widely used in mechanical engineering for creation of accurate CAD models on the basis of a physical model. Reverse engineering is useful for collecting complex geometrical features of a physical model and helpful for speeding up the modelling process. One of the means to implement RE is by using a 3D scanner to collect physical model geometry data and gather data into numerical points which together make a so-called 'point cloud', /8-10/. Reverse engineering consists of two main phases: digitalization and reconstruction. Digitization phase includes capturing the geometry data of the surface of the actual model. 3D scanners can show data in the form of point coordinates ('point cloud'), i.e. sets of polygons or images. In this case, data is collected in the form of point coordinates. The cloud of points is merged using the tessellation operation that connects adjacent points using triangles /11/.

3D scanners can be fixed to a surface, handheld or a part of automatic scanning equipment, /12/. The 3D scanner used here is a fixed device 'Geomagic Capture', Fig. 2. This device has a fixed scanning head with a rotating platform on which a physical model is placed. Total hip replacement implant is wrapped in white Teflon tape to avoid reflection, Fig. 2. Scanning is performed by recording of sections. The platform rotates and stops for the scanning head to illuminate and record the model. During scanning, the platform rotates until it makes a whole circle, and a number of sections are predefined in the software. As a software, the particular device uses an add-in for CAD package SolidWorks (Dassault Systems, France). Collected sections have to be manually merged together to resemble the scanned model. Collected data create a point cloud of a scanned hip replacement. Meshing the model into triangles is followed, applied automatically in the software. To obtain a mesh suitable for the next step, editing of the existing mesh has to be applied. Editing of the polygonal mesh

includes filtering, closing holes and surface repair from any spikes in the existing mesh. The filtered mesh is then used for the reconstruction process in CAD model, Fig. 3.

In order to estimate the accuracy of a CAD model compared to a physical model, the software has a dimensional accuracy option, Fig. 4. In this case, the point cloud is placed over a created CAD model, and colours present levels of deviation of CAD over scanned points. Blue shows the level below deviation of CAD model, and red shows the level above deviation. As Fig. 4 shows, all deviations of the CAD model are below 1 mm. CAD model is then saved in an appropriate file format (.STEP) for import in FEA software (Abaqus). Using SolidWorks, five total hip replacement implant models are made with different neck thicknesses, between original 14.6 mm and set 9 mm thickness-with 1.4 mm increments (models are with 14.6; 13.2; 11.8; 10.4; and 9 mm, respectively).



Figure 2. 3D scanning procedure of total hip replacement implant (above - device, below - physical model on scanning platform).

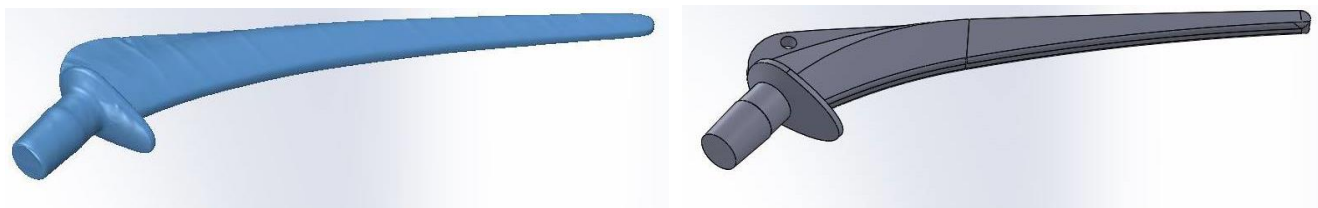


Figure 3. Digitization process (left-meshed implant, right-CAD model of the implant).

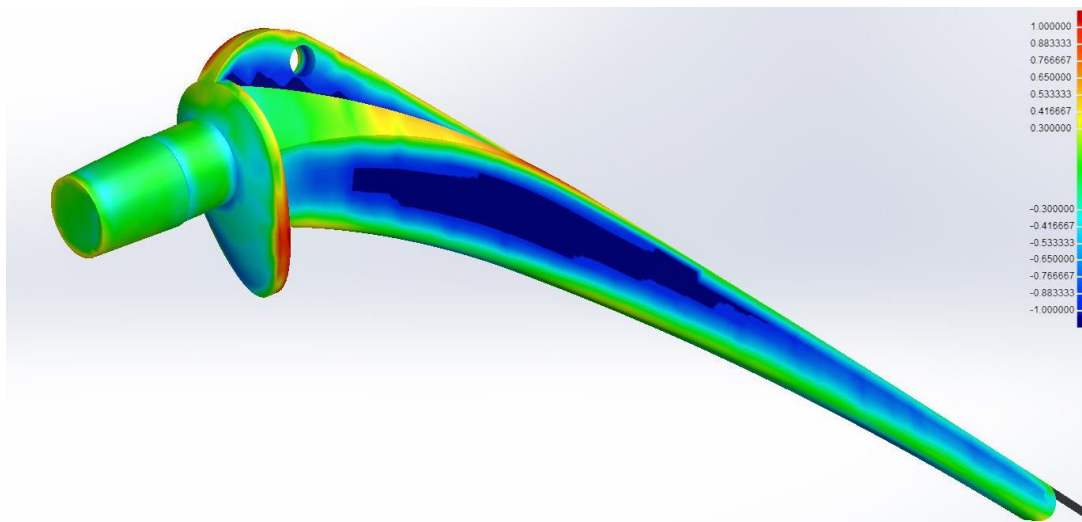


Figure 4. Deviation analysis of scanned total hip replacement implant (FEA).

Finite element analysis (FEA) is performed in Abaqus® 6.14 software (Dassault Systems, France). Two parts are imported into the software, the 3D scanned total hip replacement implant and matching implant head, 36 mm in diameter, as an assembly. The chosen implant head is made from Zirconia Y-TZP, a widely used material for stated purposes, /13/. The performed load that resembles actual load on hip joint during stumbling act, is 8.7 times the body weight of a 90 kg patient, /1/. Load is set as static, in a form of a concentrated force acting over already set reference point placed above the implant head, Fig. 5.

Surfaces between head and implant have a defined tied constraint, with head surfaces set as slave and implant surfaces set as master. Surfaces of the implant in contact with femur bone are ‘encastered’ (fixed, with no translation and rotation motion), except the bottom surface of the collar with constrained rotations of horizontal axes and vertical movement, /1/. In this particular case concentrated force equals 7681 N. Reference point is connected with a top surface of implant head by coupling constraint, enabling the load to be evenly distributed on the top surface of the implant head, /14/. Because the static loads on the total hip replacement implants result in stresses sufficiently below material yield stress, the constitutive model is set as linear elastic, /1/. In that case, only Young’s modulus and Poisson coefficient are enough for defining the material properties, as shown in Table 1.

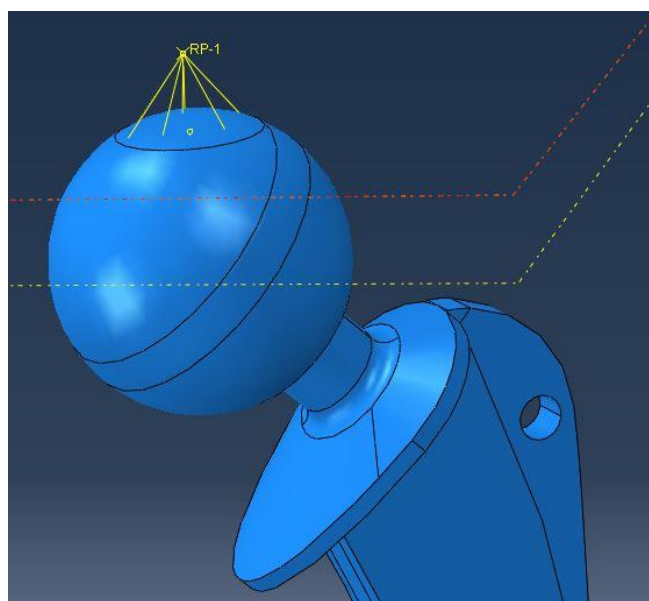


Figure 5. Reference point for concentrated force.

Table 1. Properties of Ti6Al4V ELI, Zirconia Y-TZP, /15, 16/.

Material	Young’s modulus (GPa)	Poisson coefficient
Ti6Al4V ELI	120	0.3
Zirconia Y-TZP	205	0.3

Total hip replacement implant models are meshed using a combination of linear hexahedral elements, type C3D8R, and quadratic tetrahedral elements of type C3D10. Implant head is meshed with only C3D10 elements, due to the curved geometry. Number of used elements is shown in Table 2.

All five FEA are separately meshed, resulting in a different number of nodes and elements. The total number of nodes and elements differ no more than 4 % between models, which is acceptable. The highest difference is in the total

number of used elements of the type C3D8R, which are all located in encastered areas, i.e. not relevant for FEA. Locations in the total hip replacement implant, where the stress concentrations are expected are meshed with finer elements.

Table 2. Number of used elements and nodes in meshing process.

Neck thickness (mm)	Total number of nodes	Total number of elements	C3D8R elements	C3D10 elements
14.6	494613	343517	42688	300829
13.2	497589	343019	38607	304412
11.8	507746	350101	37828	312273
10.4	512094	353006	36804	316202
9	515202	354974	36368	318606

RESULTS AND DISCUSSION

Five obtained numerical simulations show that maximal stresses are all located in the vicinity of transition area between neck and collar. Assumption taken into notice, concerning the location of the mesh refining proved to be purposeful. Stress concentrations around the boundary loca-

tion, namely between collar and stem are not taken into consideration. Due to the applied load, the implant neck exhibits a combination of tensile and compressive stresses, /1/. Neck area behind the collar of the total hip replacement implant is under tensile stresses and on the front side of the collar the compressive stresses are located. Implant neck side under tension is considered as a relevant location for a possible fatigue crack initiation site. The stress intensity and total size of the area of stress concentration in all five numerical models, of both implant neck sides, are considered in the discussion (Figs. 6-10). Stresses in these five numerical simulations are calculated according to the Von Mises stress criterion.

The original model with neck thickness of 14.6 mm, Fig. 6, has maximal stress concentration in the neck area under compressive stresses, with maximal value of 81 MPa. On the tensile side, maximal stress value is 52 MPa. The stress concentration area is wider at the back side of the implant neck, and sufficiently narrower on the front side - indicating a potential location for crack initiation.

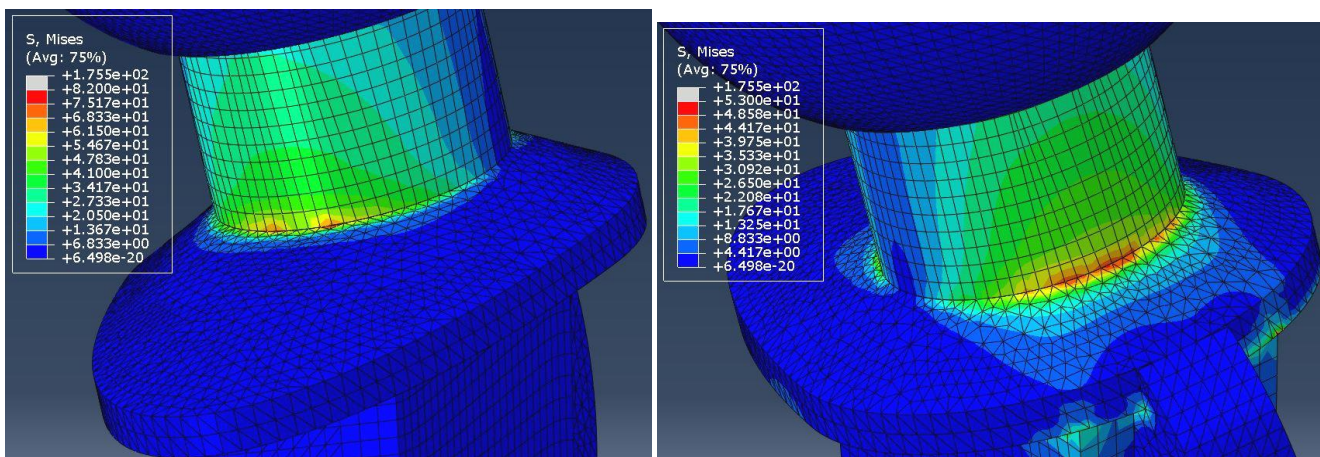


Figure 6. Total hip replacement implant with neck diameter of 14.6 mm (left-front side, right-back side).

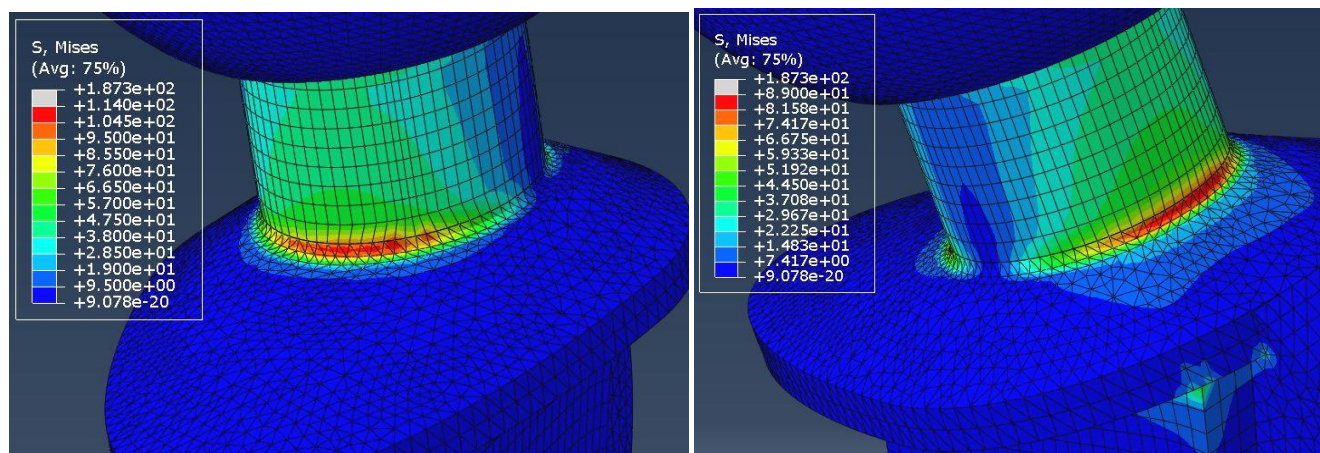


Figure 7. Total hip replacement implant with neck diameter of 13.2 mm (left-front side, right-back side).

In all five numerical simulations maximal stress concentration is set at the front side of the neck. In the first modified numerical model there is an increase in stress concentration up to 88 MPa on neck side under tension, and up to 113 MPa under compression. As shown in Fig. 7, the stress concentration area on both sides is sufficiently wider. Next

numerical model, with neck thickness of 11.8 mm, Fig. 8, has a minor increase in maximal stress values, i.e. 101 MPa on tension side and 122 MPa on the compression side of the neck, but a sufficiently thicker area of stress concentration on both sides of the implant neck. Numerical model with 10.4 mm neck thickness, Fig. 9, has an expected increase of

maximal stresses on tension and compression 128 MPa and 149 MPa, in respect. Continued narrowing and thickening of the stress concentration area on both sides is present. The last model, with recommended neck thickness of 9 mm, has highest increase of stress concentration, for both the tension and compression side, i.e. 178 MPa and 201 MPa, in respect. Area of stress concentration here is much thicker vertically and narrower horizontally (more compact), compared to the previous numerical model. The original model, according to numerical simulations, has the lowest values of maximal stress and sufficiently minor area of stress concentration, compared to other models, but due to low ergonomy represents an inappropriate solution for a patient

with higher physical daily activities. The last model provides the most satisfactory ergonomics, but a higher increase in maximal stress and much thicker and more concentrated area of stress concentration indicates the most possible unfavourable outcome of utilising the total hip replacement implant with 9 mm neck thickness. Depending on the needs of a patient and surgical evaluation in all three models, with 13.2, 11.8 and 10.4 mm, could be suitable for future use. Hence, patients with more intensive daily activities will most likely be advised for total hip replacement, using an implant with 10.4 mm thickness, and patients which have a risk of taking another hip implant operation will probably be advised to use the implant with 13.2 mm neck thickness.

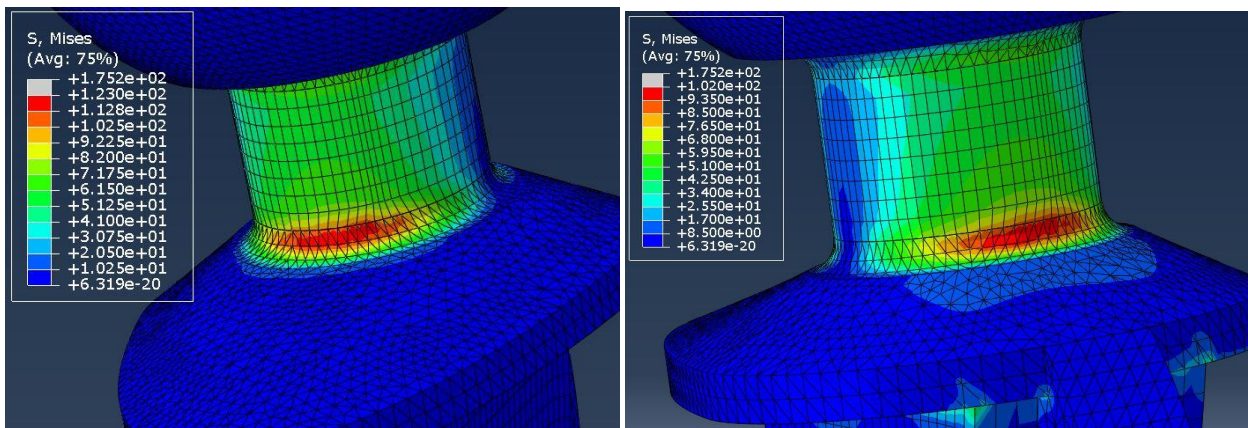


Figure 8. Total hip replacement implant with neck diameter of 11.8 mm (left-front side, right-back side)

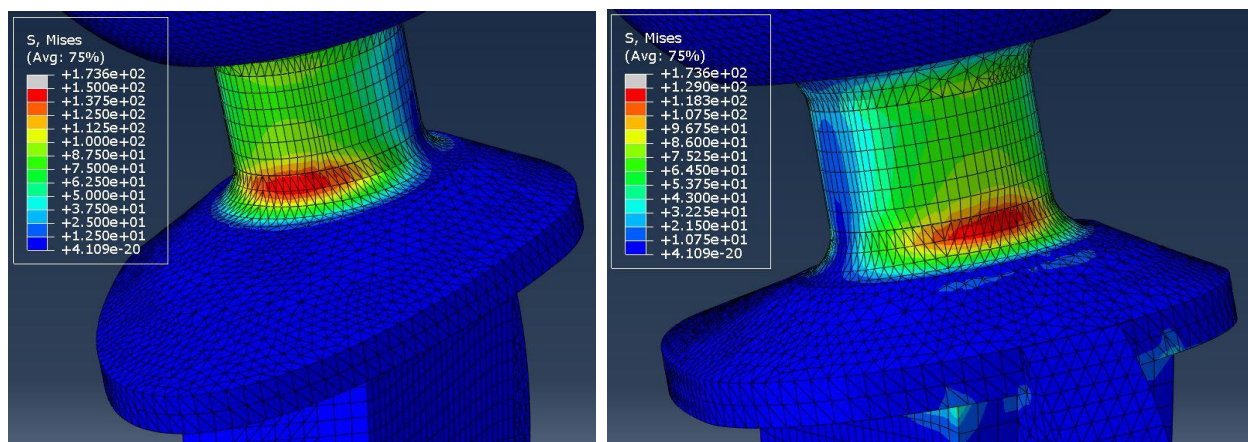


Figure 9. Total hip replacement implant with neck diameter of 10.4mm (Left-front side, Right-back side)

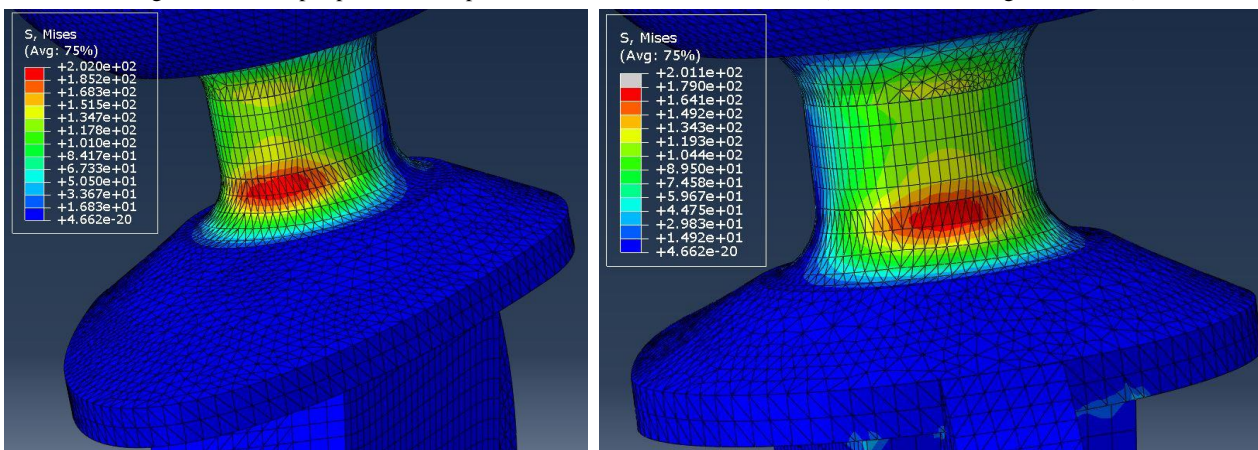


Figure 10. Total hip replacement implant with neck diameter of 9 mm (left-front side, right-back side).

CONCLUSION

This research points out the possible benefits of reverse engineering utilization in structural integrity assessment of hip replacement implants. Biomedical engineering shows tendency towards personalized therapy, medical devices and structures. Hip joint replacements are under more complex and higher loading conditions than other implant structures, which makes them the most prone to failure. Redesign of the original implant is considered only in implant neck thickness, where the highest stress concentrations are expected. Five acquired numerical simulations include appropriate implant head, and using concentrated force over the implant head results in a more accurate stress distribution around neck area under consideration. Original implant and the one with the lowest neck thickness, of the chosen five models, are presented as limiting cases-both with individual benefits over the other. Three generated models in-between are the ones of choice, depending on the patient's utilization and needs. Closed circle of 3D scanning, CAD modelling, numerical simulation (i.e. Finite Element Analysis) and manufacturing using newly developed additive technologies will present a new trend in implant manufacture. This approach to structural integrity of biomedical structures will allow a local approach to decision making, where engineers and surgeons will have influence on particular patient cases.

ACKNOWLEDGEMENTS

This research is financially supported by the Ministry of Education, Science and Technological Development of the Republic of Serbia, projects no. TR35006 and TR35040.

REFERENCES

- Milovanović, A., Sedmak, A., Čolić, et al. (2017), *Numerical analysis of stress distribution in total hip replacement implant*, Struct. Integ. & Life, 17(2): 139-144.
- Sedmak, A., Čolić, K., Burzić, Z., Tadić, S. (2010), *Structural integrity assessment of hip implant made of cobalt-chromium multiphase alloy*, Struct. Integ. and Life, 10(2):161-164.
- Čolić, K., Sedmak, A., Grbović, A., et al. (2016), *Finite element modeling of hip implant static loading*, Procedia Engng. 149: 257-262. doi: 10.1016/j.proeng.2016.06.664
- Mitrović, N., Milošević, M., Sedmak, A., et al. (2011), *Application and mode of operation of non-contact stereometric measuring system of biomaterials*, FME Trans. 39(2): 55-60.
- Sedmak, A., Čolić, K., Burzić, Z., Tadić, S. (2010), *Structural integrity assessment of hip implant made of cobalt-chromium multiphase alloy assessment of hip implant*, Struct. Integ. & Life, 10(2): 161-164.
- Sedmak, A., Milošević, M., Mitrović, N., et al. (2012), *Digital image correlation in experimental mechanical analysis*, Struct. Integ. & Life, 12(1): 39-42.
- Maehara, K., Doi, K., Matsushita, T., Sasaki, Y. (2002), *Application of vanadium-free titanium alloys to artificial hip joints*, Mater. Trans., 43(12):2936-2942. doi: 10.2320/matertrans.43.2.936
- Sokovic, M., Cedilnik, M., Kopac, J. (2005), *Use of 3D-scanning and reverse engineering by manufacturing of complex shapes*, in Proc. 13th Int. Scientific Conf. 'Achievements in Mechanical and Materials Engineering' AMME' 2005, Gliwice -Wisla, 2005: 601-604.
- Nawawi, A., Mohamed Nor, M.H., Hafiz Abdul Halim, M.A., Sidek, N.A. (2018), *The effect of surface parameters to the performance of reverse engineering process*, MATEC Web of Conf. 150, 06043, MUCET 2017. doi: 10.1051/mateconf/201815006043
- Paulic, M., Irgolic, T., Balic, J., et al. (2014), *Reverse engineering of parts with optical scanning and additive manufacturing*. Proceed. Eng. 69: 795-803. doi: 10.1016/j.proeng.2014.03.056
- Dal Maso, U., Galantucci, L. M., Percoco, G. (2006), *A volumetric approach for layered manufacturing of scattered point clouds*, in Proc. AMPT 06 - Advances in Materials and Processing Technologies, Las Vegas, USA, 2006.
- Shabani, B., Vrtanoski, G., Dukovski, V. (2018), *Integrated reverse engineering and additive technology systems*, Mech. Eng. - Sci. J, 36(1): 47-54.
- Tsikandylakis, G., Mohaddes, M., Cnudde, P., et al. (2018), *Head size in primary total hip arthroplasty*. EFORT Open Rev. 3(5): 225-231. doi: 10.1302/2058-5241.3.170061
- Babić, M., Verić, O., Božić, Ž., Sušić, A. (2019), *Fracture analysis of a total hip prosthesis based on reverse engineering*, Engineering Fracture Mechanics 215: 261-271. doi: 10.1016/j.engfracmech.2019.05.003
- Hosseini, S., *Fatigue of Ti-6Al-4V*, in: Biomedical Engineering - Technical Applications in Medicine, Ed. by R. Hudak, M. Penhaker, J. Majernik, InTech, Rijeka, Croatia 2012. doi: 10.5772/45753
- Luthardt, R.G., Holzhüter, M., Sandkuhl, O., et al. (2002), *Reliability and properties of ground Y-TZP-zirconia ceramics*, J Dent. Res. 81: 487-491. doi: 10.1177/154405910208100711

© 2019 The Author. Structural Integrity and Life. Published by DIVK (The Society for Structural Integrity and Life 'Prof. Dr Stojan Sedmak') (<http://divk.inovacionicentar.rs/ivk/home.html>). This is an open access article distributed under the terms and conditions of the [Creative Commons Attribution-NonCommercial-NoDerivatives 4.0 International License](https://creativecommons.org/licenses/by-nc-nd/4.0/)